Analyst

Accepted Manuscript

ROYAL SOCIETY OF CHEMISTRY

www.rsc.org/analyst

Square-wave adsorptive stripping voltammetric determination of nanomolar levels of bezafibrate using a glassy carbon electrode modified with multi-walled carbon nanotubes within a dihexadecyl hydrogen phosphate film

Jorge Armando Ardila[a], Geiser Gabriel Oliveira[b], Roberta Antigo Medeiros[c] and Orlando Fatibello-Filho[a,d*]

[a]Departamento de Química, Universidade Federal de São Carlos, C.P. 676, CEP 13.560-970, São Carlos – SP, Brazil

[b]Instituto de Química de São Carlos, USP – Universidade de São Paulo, C.P. 780, CEP 13.560-970, São Carlos – SP, Brazil

[c]Centro de Engenharias e Ciências Exatas, Universidade do Oeste do Paraná, CEP 85903-000, Toledo – PR, Brazil

[d]Instituto Nacional de Ciência e Tecnologia de Bioanalítica (INCT de Bioanalítica)

*Corresponding author. Tel.: +55-16-33518098; Fax +55-16-33518350

e-mail: bello@ufscar.br (O. Fatibello-Filho)

A**bstract**

A highly sensitive method for bezafibrate determination using a glassy carbon electrode (GCE) modified with multi-walled carbon nanotubes within a dihexadecyl hydrogen phosphate film based on a square-wave adsorptive stripping voltammetry (SWAdSV) is proposed. The electrochemical behaviour of bezafibrate has been studied by cyclic voltammetry, showing an irreversible anodic peak at a potential of 1.09 V in 0.1 mol L^{-1} phosphate buffer solution (pH 2.0). A study of the scan rate showed that the oxidation of bezafibrate is an adsorptive-controlled process, involving the transfer of two electrons and two protons per molecule. The analytical curve was linear over a bezafibrate concentration range from 50 to 910 nmol L^{-1}, with a detection limit of 16 nmol L^{-1}. This analytical method was successfully applied for benzafibrate determination in pharmaceutical formulations, with results that showed good agreement with those obtained using a comparative spectrophotometric method and has the potential for field application.

Keywords: benzafibrate determination, glassy carbon electrode, modified electrode, multi-walled carbon nanotubes (MWCNTs), anodic square-wave adsorptive stripping voltammetry (SWAdSV).

1. Introduction

Carbon nanotubes (CNTs) are allotropes of carbon with a cylindrical nanostructure discovered by Iijima in 1991[1-3]. Some of their amazing and unique properties such as high electrical conductivity, high surface area, good mechanical strength and excellent thermal and chemical stability have received intense attention in the field of new electrochemical sensors and biosensors[4-7]. Nevertheless, the major problem for developing CNT-based sensors is their low solubility in solvents such as ethanol, methanol, isopropanol and water. However, functionalization of these CNTs can promote modification of the chemical structure and is the most frequently employed strategy to improve the dispersal of CNTs in aqueous solution[6,8,9]. Many investigators have extensively studied their chemical functionalization. The results reported in different studies showed that oxidation with strong acids (hydrochloric, sulphuric and nitric acid or mixtures thereof) are the most effective treatment for CNT activation. This treatment inserts oxygen groups (phenols, carboxylic and sulphonic acids, nitro etc) into tube ends and defect sites[10] and promotes the generation of hydrophilic functional groups that can in turn realize hydrogen bonds between the CNTs and the solvent to increase the CNTs' solubility. Moreover, treatment with strong acids removes impurities such as the metal catalyst[11] and amorphous carbon on the inner and outer surfaces of CNTs.

The use of CNTs for sensor fabrication has become the focus of many scientific research studies, due to their high electronic conductivity for the electron transfer reactions and better electrochemical and chemical stabilities in both aqueous and non-aqueous solutions, selectivity and sensitivity. CNTs has been using in the fabrication of modified electrodes for adsorptive stripping measurements for the quantification of nanomolar levels of pharmaceutical compounds[12-14]. Several applications of modified

CNT-based electrodes have been reported based on the dispersal of CNTs in solutions containing compounds such as

dihexadecyl hydrogen phosphate (DHP), poly(allylamine) hydrochloride (PAH), Nafion, ionic liquid, nanoparticles, chitosan and multiples organic and biologic compounds[15-23]. These modifying agents increase the dispersal of CNTs in aqueous media and, moreover, help to immobilize the CNTs on the electrode surface, avoiding loss of the film during measurements. Thus, is easy to elaborate electroactive films by a simple drop coating procedure. DHP, used in this work, is an anionic surfactant with two hydrophobic C-H chains that has been used as a modifying agent in the preparation of stable aqueous dispersals of functionalized CNTs for the fabrication of electrochemical sensors by drop coating on solid electrodes[24-27].

Fibrates are pharmaceuticals highly effective for the treatment of patients with hyperlipidemia. Actually, many fibric acids such as ciprofibrate, clofibrate, gemfibrozil fenofibrate and bezafibrate are commonly used as antihyperlipidemic agents[28,29]. Bezafibrate (BZF), 2-[4-[2-[(4-chlorobenzoyl)amino] ethyl]phenoxy]-2-methylpropanoic acid is a fibrate agonist of the peroxisome proliferator receptor selective for α receptors (PPAR- α) that potently decreases plasma low density lipoprotein (LDL) and increases serum high-density lipoprotein (HDL) levels in the blood, significantly reducing the risk of major cardiac events[30].

To ensure treatment efficacy it is necessary to control the quality of pharmaceutical products through accurate determinations of BZF in the raw material and finished formulations. Moreover, for pharmacokinetic studies it is also necessary to use sensitive analytical methods that allow determinations at the nanomolar level. Thus, several analytical methods have been reported for evaluating BZF in pharmaceutical

products and biological fluids. BZF is generally determined by capillary electrophoresis[31], chromatography[32-35] and spectrophotometry[35]. Voltammetric methods are a good alternative, since these methods have high sensibility and very low detection limits, the instrumentation is economic, little or no sample pretreatment is necessary and additional information can be obtained such as the number of electrons and protons transferred in the reaction. There is currently only one voltammetric method for BZF determination using a boron-doped diamond as working electrode electrode[36]. The analytical curve was linear in the concentration range 0.10 – 9.1 μmol L^{-1} with a detection limit of 0.098 μmol L^{-1}.

In this work, we report on the fabrication of a glassy carbon electrode (GCE) modified with multi-walled carbon nanotubes (MWCNTs) within a DHP film for the determination of BZF in pharmaceutical formulations by anodic square-wave adsorptive stripping voltammetry (SWAdSV). This proposed method is simple and fast and allowed determinations of this analyte at nanomolar levels with a detection limit of 16 nmol L^{-1}, lower than that reported previously by our research group using a boron-doped diamond electrode[36].

2. Experimental

2.1. Reagents and Solutions

Bezafibrate, dihexadecyl hydrogen phosphate and multi-walled carbon nanotubes (20 – 30 nm in diameter and 0.5 – 2.0 μm in length; purity: ≥ 95 %) were purchased from Sigma-Aldrich. The supporting electrolyte was a 0.1 mol L^{-1} phosphate buffer solution (pH 2.0). A stock solution of 1.0×10^{-3} mol L^{-1} BZF was freshly prepared in pure ethanol and working solutions were prepared by dilution of the stock solution with supporting electrolyte. All chemicals were of analytical-reagent grade and

all solutions were prepared using ultra-purified water (resistivity greater than 18 MΩ cm) supplied by a Milli-Q system (Millipore®).

2.2 Apparatus

All voltammetric measurements were carried out using an Autolab PGSTAT-30 (Ecochemie) potentiostat/galvanostat controlled with GPES 4.9 or FRA software. A three-electrode cell was employed, using a platinum wire as counter electrode, Ag/AgCl (3.0 mol L^{-1} KCl) as reference electrode and either a GCE (3.8 mm diameter) or a dihexadecyl hydrogen phosphate modified glassy-carbon electrode (DHP/GCE) or a dihexadecyl hydrogen phosphate/multi-walled carbon nanotube modified glassy-carbon electrode (MWCNT-DHP/GCE) as the working electrode. The electrochemical impedance spectroscopy (EIS) experiments were performed at the formal potential of the $K_4Fe(CN)_6$ / $K_3Fe(CN)_6$ redox pair, from 10 mHz to 100 kHz (10 points per decade) and with a 10 mV (r.m.s.) ac perturbation, for 1.0 mmol L^{-1} $K_4Fe(CN)_6$ in a 0.5 mol L^{-1} KCl solution.

2.3 Preparation of working electrode

To prepare the proposed MWCNT-DHP/GCE, 100 mg of the MWCNTs were purified by mixing with 50 mL of 2.0 mol L^{-1} HCl and stirring for 12 h, followed by washing several times with ultrapure water. After this, the MWCNTs were functionalized chemically in a mixture of 50 mL of concentrated sulphuric acid and nitric acid (3:1 v/v) for 12 h at room temperature. The MWCNTs were washed with deionized water several times until the wash reached pH 6.5–7.0 and separated by

centrifuging. The solid collected in the bottom of the centrifuge tube was dried at 120 °C for 6 h.

The MWCNT-DHP film was prepared by sonicating 1 mg of functionalized MWCNTs and 1 mg DHP in 1 mL of ultrapure water for 120 min. Thus, a stable and homogeneous black dispersion was obtained. A volume of 15 µL was dipped on the surface of a GCE previously polished to a mirror finish using an ultrafine abrasive paper and 1.0 µm and 0.5 µm of alumina slurry. After 2 h at room temperature, the solvent was dry and a uniform MWCNT-DHP film was formed on the GCE surface.

2.4 General Analytical Procedure

Initially, a pre-treatment of the MWCNT-DHP/GCE surface was carried out by cyclic voltammetry. For this, 50 scans in the potential window from –0.2 to 1.4 V (*vs.* Ag/AgCl (3.0 mol L^{-1} KCl)) at a potential scan rate (ν) of 50 mV s^{-1} in 10 mL of 0.1 mol L^{-1} phosphate buffer solution (pH 2.0) were realized. This pretreatment promoted a decrease in the capacitive current of the background current of this electrode. Then, in another conventional glass cell containing 10 mL of 0.1 mol L^{-1} phosphate buffer solution (pH 2.0) and the pretreated MWCNTs-DHP/GCE as working electrode, the BZF quantification was carried out. The BZF was accumulated at open-circuit potential for 180 s. The square-wave adsorptive stripping voltammetric (SWAdSV) parameters used were: square-wave frequency (*f*) of 20 Hz, pulse amplitude (*a*) of 40 mV and scan increment (*ΔEs*) of 7 mV. The anodic peak current was measured at 1.09 V. After optimizing the experimental parameters for the proposed method, an analytical curve was constructed by adding small volumes of a standard BZF solution to the supporting electrolyte solution (0.1 mol L^{-1} phosphate buffer solution (pH 2.0)).

2.5 Sample preparation

Ten tablets (40 mg BZF/tablet) were accurately weighed and powdered in a mortar. An accurately weighing amount of powder was transferred into a 50 mL calibrated flask and 25 mL of ethanol was added. The sample contained in the flask was then sonicated for 30 min to complete dissolution, then the volume in the flask was completed to the volume with ethanol. Afterward, an appropriate aliquot was diluted with supporting electrolyte.

A 10 mL volume of 0.1 mol L^{-1} phosphate buffer solution (pH 2.0) was introduced into the voltammetric cell and a suitable volume of the sample solution was added. The determination of BZF was carried out using a standard addition method.

3. Results and Discussion

3.1. Characterization of the electrodes by electrochemical impedance spectroscopy

EIS is a powerful tool for studying interfacial properties of surface-modified electrodes[37,38]. It was performed to provide information on changes in the electrode surface during the modification process. A typical impedance spectrum, namely, the Nyquist plot, includes a semicircular portion at higher frequencies whose diameter equals the electron transfer resistance (R_{et}), and a linear portion at lower frequencies, representing the diffusion-limited process (mass transfer control). As shown in Figure 1, the difference between the EIS diagrams on the bare GCE and on the modified electrodes was evident. The bare GCE displayed a larger semicircle with a R_{et} of 1.82 kΩ, indicating the poorer electron transfer kinetics of $K_4Fe(CN)_6$ on the GCE. When DHP was deposited on the surface of the GCE, the R_{et} increased to 5.23 kΩ. This phenomenon could be attributed to the DHP film itself, which introduces a resistance

into the electrode/solution system and/or to a decrease in $K_4Fe(CN)_6$ diffusion through the DHP film. However, with the introduction of MWCNTs into the electrode (MWCNT-DHP/GCE), the electron resistance decreased to 1.0 kΩ. A semicircle smaller than that observed with bare GC electrode suggested that the MWCNTs increased the electron transfer rate on the electrode surface.

In addition, the standard heterogeneous rate constant for each electrode was calculating according to Eq. 1:

$$k^0 = \frac{RT}{F^2 R_{et} AC} \quad (1)$$

where k^0 is the standard heterogeneous electron transfer rate constant (cm s^{-1}), R_{et} is the electron transfer resistance (Ω) obtained in the EIS experiments that was determined as the diameter of the high-frequency semicircle in the impedance complex-plane plots, A is the electrode surface area (cm^2), C is the concentration of the $K_4[Fe(CN)_6]$ solution (1.0×10^{-6} mol cm^{-3}) and the other symbols have their conventional meanings. The k^0 values obtained for the GC, DHP/GC and MWCNTs-DHP/GC electrodes were 4.76×10^{-3}, 2.49×10^{-3} and 1.37×10^{-2} cm s^{-1}, respectively. The value of k^0 is a measure of the kinetic facility of a redox pair. A system with a large k^0 value will achieve equilibrium on a short time scale and a system with a small k^0 value will be sluggish. Thus, with the MWCNT-DHP/GCE the k^0 value is larger, indicating faster transfer of electrons in this electrode when compared with the other electrodes, GCE and DHP/GCE.

Figure 1

3.2. Electroactive surface area

SEM characterization of MWCNT-DHP/GCE surface was previously carried out by our research group and the results were discussed as described elsewhere[14]. The electroactive surface areas for the bare GCE, DHP/GCE and MWCNT-DHP/GCE were estimated by using the Randles-Ševćik equation (Eq. 2). This equation describes the variation in the anodic peak current (I_{ap}) as a function of the square root of the potential scan rate ($v^{1/2}$) by the following expression [39]:

$$I_{ap} = (2.69\times10^{5})n^{3/2}AD^{1/2}\,Cv^{1/2} \quad (2)$$

where n is the total number of electrons transferred during the overall electrochemical process, A is the electrode surface area (cm^2), D is the diffusion coefficient of the reduced species ($cm^2\ s^{-1}$), and C is the reduced species concentration (mol cm^{-3}). Cyclic voltammograms for 1.0 mmol L^{-1} $K_4[Fe(CN)_6]$ ($D = 6.2 \times 10^{-6}$ $cm^2\ s^{-1}$)[40] in a 0.1 mol L^{-1} KCl solution were obtained using these three electrodes, as shown in the supplementary material file in Figure SM-1. A linear relationship was observed between the anodic peak current and the scan rate (0.010 to 0.300 V s^{-1}) for the three electrodes. Using the slope of this linear relationship for the bare GCE, DHP/GCE and MWCNT-DHP/GCE and the Randles-Ševćik equation, the electroactive surface areas were calculated as 0.086, 0.014 and 0.111 cm^2, respectively. These results indicated that the electroactive surface area increased after modifying the GCE with the MWCNT-DHP film. The presence of MWCNTs on the electrode's surface yielded an increase in the intensity of the peak current, a decrease in the detection limit and an increase in sensitivity.

3.3 Voltammetric behavior of BZF

The electrochemical response obtained for 300 nmol L^{-1} BZF in 0.1 mol L^{-1} phosphate buffer solution (pH 2.0) was evaluated and compared using the bare GCE, DHP/GCE and MWCNT-DHP/GCE (see Figure 2). With the CGE, the BZF oxidation potential obtained was 1.13 V, with a peak current of 1.9 μA and a broad base, which may decrease the selectivity of the method. For the DHP/GCE, no BZF oxidation peak was observed due to blockage of the electrode surface by the polymeric film. On the other hand, using the MWCNT-DHP/GCE a well-defined BZF oxidation peak was obtained, with a peak current of 71.5 μA and an oxidation potential of 1.09 V, 40 mV more negative than with the GCE. The increase in the peak current and decrease in the potential of BZF oxidation may be ascribed to the presence of MWCNTs on the electrode surface. This electroactive film improves the electrochemical response due to its excellent electrochemical characteristics, such as good electrical conductivity, high chemical stability and high surface area. Moreover, no reduction peak for BZF was observed, indicating that BZF oxidation is an irreversible charge-transfer process.

Figure 2

In addition, the effect of different supporting electrolytes (0.1 mol L^{-1} acetic buffer solution (pH 4.5), 0.1 mol L^{-1} phosphate buffer solution (pH 2.0), Britton-Robinson buffer solution (pH 2.0), and 0.1 mol L^{-1} H_2SO_4) on the electrochemical response of BZF were studied by cyclic voltammetry. As can be seen in Figure SM-2, the best response (highest peak current signal with well-defined peaks) was obtained using a 0.1 mol L^{-1} phosphate buffer solution (pH 2.0). Then, different pH values for

the phosphate buffer solutions were evaluated (see Figure 3). The maximum electrochemical response and well-defined redox peak was obtained at pH 2.0. Therefore, phosphate buffer solution (pH 2.0) was chosen as the supporting electrolyte for further experiments.

Figure 3

Figure 3 also shows that the BZF oxidation potential decreases with increasing pH, indicating that the pH of the supporting electrolyte is a determinant in BZF oxidation. The regression equation that described this behaviour can be expressed as E_p (V) = 1.201 − 0.051 pH (R = 0.997). Through the use of Eq. 3 [41]:

$$E_p = E^0 - 2.303\left(\frac{mRT}{nF}\right)pH \quad (3)$$

where E_p is the electrode potential, E^0 is the standard electrode potential, m is the number of protons, n is the number of electrons transferred in the electrochemical reaction, and the other symbols have their usual meanings. The slope value of −51.0 mV per pH unit is close to the theoretical slope (−59.2 mV per pH unit at 298.15 K) [41]. This clearly shows that equal numbers of electrons and protons are involved in the electro-oxidation of BZF at the MWCNT-DHP/GCE. It means that not only electrons but also protons are released from the BZF molecule during oxidation. This result is in agreement with a previous report in the literature[42] (additional information about the BZF oxidation mechanism will be presented in section 3.5).

The stability of the MWCNT-DHP/GCE was tested with 30 μmol L^{-1} BZF in phosphate buffer solution (pH 2.0). The cyclic voltammetric responses were constant

during 50 cycles indicating that the BZF adsorption is reversible, after which the response decreased *ca* 5 % compared with the initial response, likely due to poisoning of electrode surface and/or loss of a small quantity of MWCNTs from the electrode's surface. That number of measurements per polymeric film was sufficient for one or more workdays. Moreover, when necessary, a new film could be easily prepared as described in section 2.3 using the same MWCNTs-DHP dispersion.

.

3.4. Influence of adsorption time on the response of BZF

With the aim of increasing the sensitivity of BZF determination, the adsorption potential and adsorption time were explored. The adsorption potential had no effect on the peak current for 30 μmol L^{-1} BZF in phosphate buffer solution (pH 2.0) over a potential range from –0.1 to 0.8 V. This electrochemical behaviour leads to the conclusion that the potential applied on the working electrode had no effect on the accumulation of BZF on the MWCNT-DHP/GCE. Therefore, the accumulation of BZF was performed under an open-circuit.

Next, we studied the effect of the adsorption time for 30 μmol L^{-1} BZF in phosphate buffer solution (pH 2.0) on the MWCNT-DHP/GCE. The peak current of BZF increased greatly when the adsorption time increased in the range from 30 to 180 s, as can be seen in Figure SM-3. At times longer than 180 s the peak current intensity remained constant. Thus, the adsorption time employed in subsequent studies was 180 s, this adsorption is reversible as discussed in section 3.3.

3.5. Effect of scan rate

The effect of the scan rate (v) on the electrochemical behaviour of BZF was investigated using the MWCNTs-DHP/GCE and linear sweep adsorptive stripping voltammetry. Figure 4 shows the linear sweep voltammograms for 30 μmol L^{-1} BZF in phosphate buffer solution (pH 2.0) obtained at different scan rates (0.01 □ 0.20 Vs^{-1}). A linear relationship was observed between the oxidation peak current and v, with a significant correlation coefficient of 0.998 and represented by the equation: $I_p = 7.8 \times 10^{-9} v + 3.4 \times 10^{-7}$.

Figure 4

A plot of the log of the peak current (log I_{ap}) *vs.* the log of the scan rate (log v) (see Figure SM-4) gives a slope of 0.991. This is close to the theoretical value of 1.0 reported for an ideal reaction for an adsorption-controlled electrode [39]. Additionally, the relationship between the BZF oxidation potential and the scan rate was investigated. The results presented in the insert of Figure 4 show a linear relationship represented by the equation: E_p (V) = 0.029 ln$v$ (V s^{-1}) + 1.165, r = 0.998. The peak potential (E_p) is a linear function of the log of v, in agreement with Laviron's theory for an irreversible electrode process. According to Laviron's theory [43]:

$$E_p = E^0 - \left(\frac{RT}{\alpha nF}\right)\ln\left(\frac{RTk_S}{\alpha nF}\right) + \left(\frac{RT}{\alpha nF}\right)\ln v \qquad (5)$$

where E^0 is the formal redox potential, α is the charge transfer coefficient, n is the number of electrons transferred, k_s is the heterogeneous electron transfer rate constant, and v is the scan rate. Other symbols have their usual meanings. Thus, the αn value was

easily calculated from the slope of E_p *vs.* ln$v$ plot; the αn value calculated was 0.90. Generally, α is assumed to be 0.5 in a totally irreversible electrode process. Thus, the number of electrons transferred in the electro-oxidation of BZF was calculated to be 1.8 (approximately equal to 2). Therefore, the electrochemical mechanism of electro-oxidation of BZF involves the transfer of two electron and two protons, supported by the results obtained in the study of the pH effect (see Figure 5). These results are in agreement with the BZF oxidation mechanism proposed in the literature[36, 42].

Figure 5

3.6 Assessment of analytical parameters of the proposed method for BZF determination

First, the experimental parameters that affect the SWAdSV responses were optimized for 300 nmol L^{-1} BZF in phosphate buffer solution (pH 2.0). For square-wave voltammetry the range of values investigated were: 10 – 50 s^{-1}, for the square-wave frequency (f); 10 – 60 mV, for the pulse amplitude (a); 1 – 7 mV, for the scan increment (ΔE_s). The values selected were: f = 20 s^{-1}, a = 40 mV, and ΔE_S = 7 mV.

Then, the optimized instrumental and experimental parameters were employed to record an analytical curve for BZF. SWAdS voltammograms were obtained for different BZF concentrations, from 50 to 910 nmol L^{-1}, as shown in Figure 6. The peak current as a function of BZF concentration produces a straight line and the linear plot can be expressed by Equation 6:

$$I_{ap}\ (\mu A) = 0.078 + 3.4 \times 10^{-3}\ c\ (\text{nmol L}^{-1});\ r = 0.998 \quad (6)$$

where I_{ap} is the anodic peak current and c is the BZF concentration. Additionally, the limit of detection (*LOD*) was calculated using the formula 3S/M, where S is the standard deviation of ten measurements of the blank solution and M is the slope of the analytical curve. As shown in Table 1, the LOD obtained using the proposed voltammetric method was 16 nmol L^{-1}. This value is lower than those obtained employing other analytical methods for BZF determination using different techniques[32-36] and 6 times lower than the value using the unique voltammetric method for BZF determination found in the literature using a boron-doped diamond electrode[36] and 1.7 times lower than the LOD obtained using a HPLC[34] method.

Figure 6

Table 1

The intra and inter-day repeatability of the proposed method for BZF determination using the MWCNT-DHP/GCE was also evaluated. For intra-day repeatability, 10 successive measurements were performed for a 500 nmol L^{-1} BZF solution. The relative standard deviation (RSD) obtained was 3.8%. For inter-day repeatability, 500 nmol L^{-1} BZF solutions were used to perform measurements during 5 consecutive days, maintaining the same conditions. The RSD obtained was 4.8%. This result shows that using the MWCNT-DHP/GCE and SWAdSV, BZF determination can be performed with adequate repeatability even at extremely low levels.

With the aim of assessing the selectivity of the proposed method, the influence of some concomitant compounds was studied. The potential interfering substances (magnesium stearate, starch, polyvinyl alcohol and methylcellulose) were chosen from the group of substances commonly found with BZF in pharmaceutical formulation

samples. Thus, SWAdS voltammograms for 500 nmol L^{-1} BZF in 0.1 mol L^{-1} phosphate buffer solution (pH 2.0) were obtained in the presence of possible interferents at concentration ratios of 1:1 and 1:10 (BZF solution:interferent). The difference in the intensity of the oxidation peak current was ± 4.5 % when the oxidation peak current of the BZF solution was compared with the oxidation peak current of BZF in the presence of the interferents. Thus, we concluded that these compounds do not significantly interfere with the determination of BZF under the experimental conditions used.

Recovery experiments also were carried out to evaluate matrix effects. The study was realized by adding known aliquots of a standard BZF solution into a known volume of sample present in the supporting electrolyte. The recoveries obtained for BZF in the analysed pharmaceutical formulations varied between 94.5 and 104 %, clearly indicating that the proposed method does not suffer from any significant effects of matrix interference.

In order to evaluate the analytical applicability of the proposed method, it was used to determine BZF in pharmaceutical formulation samples. The results obtained are shown in Table 1 together with the results obtained with a spectrophotometric method for comparison[35]. As can be seen in this table, no significant differences were observed between the values found for the content of BZF in the tablets using the proposed voltammetric method and the comparative one. The results in this table were also compared statistically by applying the paired *t*-test[44]. The value of t calculated (2.4) was smaller than the critical one (3.2, $\alpha = 0.05$), indicating that the results obtained with either method are not statistically different, at a 95% confidence level. Thus, the modified electrode retained its efficiency for determining BZF in pharmaceutical formulation samples with satisfactory results.

Table 2

4. Conclusions

In this study, we have successfully fabricated a modified GCE using carbon nanotubes and dihexadecyl hydrogen phosphate film by a simple drop coating procedure. The MWCNT-DHP/GCE was applied to the electrochemical characterization and electroanalytical determination of BZF at extremely low concentrations by SWAdSV. The results showed that the intensity of the BZF oxidation peak current was significantly increased when the MWCNTs were dropped onto the GCE, making it possible to develop a highly-sensitive voltammetric method. The proposed method presented a lower detection limit (16 nmol L^{-1}), a linear range (50 □ 910 nmol L^{-1}), and an average error between –2.9 and 0.5% when compared with a spectrophotometric method for pharmaceutical formulation analysis. Furthermore, the results presented here allow us to conclude that the combination of SWAdSV and a MWCNT-DHP/GCE is a simple, rapid and inexpensive alternative for analytical determinations of BZF in pharmaceutical formulations.

Acknowledgements

The authors gratefully acknowledge the financial support from the Brazilian funding agencies FAPESP (Proc. 2011/00601-9), CNPq, CAPES, and INCT-Bioanalítica.

References

1. H. Y. Niu, X. Q. Chen, S. B. Wang, D. Z. Li, W. D. L. Mao and Y. Y. Li, *Phys. Rev. Lett.*, 2012, **108**, 135501.
2. A. Hirsch, *Nat. Mater.*, 2010, **9**, 868-871.
3. S. Iijima, *Nature*, 1991, **354**, 56-58.
4. B. C. Janegitz, R. Pauliukaite, M. E. Ghica, C. M. A. Brett and O. Fatibello-Filho, *Sens. Actuators B: Chem.*, 2011, **158**, 411-417.
5. A. Afkhami and H. Ghaedi, *Anal. Methods*, 2012, **4**, 1415-1420.
6. E. Bekyarova, M. Davis, T. Burch, M. E. Itkis, B. Zhao, S. Sunshine and R. C. Haddon, *J. Phys. Chem. B*, 2004, **108**, 19717-19720.
7. C. E. Banks and R. G. Compton, *Analyst*, 2006, **131**, 15-21.
8. V. Datsyuk, M. Kalyva, K. Papagelis, J. Parthenios, D. Tasis, A. Siokou, I. Kallitsis and C. Galiotis, *Carbon*, 2008, **46**, 833-840.
9. G. G. Oliveira, E. R. Sartori, H. H. Takeda and O. Fatibello-Filho, *Chem. Sens.*, 2012, **2**, 1-7.
10. S. Santangelo, G. Messina, G. Faggio, S. H. A. Rahim and C. Milone, *J. Raman Spectrosc.*, 2012, **43**, 1432-1442.
11. K. Jurkschat, X. Ji, A. Crossley, R. G. Compton and C. E. Banks, *Analyst*, 2007, **132**, 21-23.

12. R. T. Kachoosangi, G. G. Wildgoose and R. G. Compton, *Anal Chim Acta*, 2008, **618**, 54-60.

13. R. T. Kachoosangi, G. G. Wildgoose and R. G. Compton, *Electroanalysis*, 2008, **20**, 1714-1718.

14. G. G. Oliveira, B. C. Janegitz, V. Zucolotto and O. Fatibello-Filho, *Central European Journal of Chemistry*, 2013, **11**, 1837-1843.

15. B. Sljukic, C. E. Banks and R. G. Compton, *Nano letters*, 2006, **6**, 1556-1558.

16. B. Sljukic, C. E. Banks, C. Salter, A. Crossley and R. G. Compton, *Analyst*, 2006, **131**, 670-677.

17. E. R. Sartori, H. H. Takeda and O. Fatibello-Filho, *Electroanalysis*, 2011, **23**, 2526-2533.

18. B. C. Janegitz, L. H. Marcolino, S. P. Campana, R. C. Faria and O. Fatibello-Filho, *Sens. Actuators B: Chem.*, 2009, **142**, 260-266.

19. T. Tavana, M. A. Khalilzadeh, H. Karimi-Maleh, A. A. Ensafi, H. Beitollahi and D. Zareyee, *J. Mol. Liq.*, 2012, **168**, 69-74.

20. Y. B. Zeng, D. J. Yu, Y. Y. Yu, T. S. Zhou and G. Y. Shi, *J. Hazard. Mater.*, 2012, **217**, 315-322.

21. A. Mandil, R. Pauliukaite, A. Amine and C. M. A. Brett, *Anal. Lett.*, 2012, **45**, 395-407.

22. M. E. Ghica, R. Pauliukaite, O. Fatibello-Filho and C. M. A. Brett, *Sens. Actuators B: Chem.*, 2009, **142**, 308-315.

23. H. H. Takeda, B. C. Janegitz, R. A. Medeiros, L. H. C. Mattoso and O. Fatibello-Filho, *Sens. Actuators B: Chem.*, 2012, **161**, 755-760.

24. D. Sun and H. J. Zhang, *Anal. Chim. Acta*, 2006, **557**, 64-69.

25. W. S. Huang and C. H. Yang, *Anal. Lett.*, 2007, **40**, 3280-3289.

26. D. Y. Zheng, X. J. Liu, D. Zhou and S. S. Hu, *Microchim. Acta*, 2012, **176**, 49-55.

27. L. L. C. Garcia, L. C. S. Figueiredo-Filho, G. G. Oliveira, O. Fatibello-Filho and C. E. Banks, *Sens. Actuators B: Chem.*, 2013, **181**, 306-311.

28. S. Abourbih, K. B. Filion, L. Joseph, E. L. Schiffrin, S. Rinfret, P. Poirier, L. Pilote, J. Genest and M. J. Eisenberg, *Am J Med*, 2009, **122**, 962.

29. S. R. Freeman, A. L. Drake, L. F. Heilig, M. Graber, K. McNealy, L. M. Schilling and R. P. Dellavalle, *J. Natl. Cancer I*, 2006, **98**, 1538-1546.

30. J. Lee, S. Balakrishnan, J. Cho, S. H. Jeon and J. M. Kim, *J Mater Chem*, 2011, **21**, 2648-2655.

31. Ł. Komsta, G. Misztal, E. Majchrzak and A. Hauzer, *J. Pharm. Biomed. Anal.*, 2006, **41**, 408-414.

32. L. D. Masnatta, L. A. Cuniberti, R. H. Rey and J. P. Werba, *J Chromatogr B*, 1996, **687**, 437-442.

33. W. Zhang, B. R. Xiang, Y. Zhan, L. Y. Yu, T. Wang and C. Y. Wang, *J. Chromatogr. Sci.*, 2008, **46**, 844-847.

34. J. de Melo, F. K. Hurtado, F. S. Poitevin, F. C. Flores, E. S. Zimmermann, S. L. Dalmora and C. M. B. Rolim, *J. Chromatogr. Sci.*, 2010, **48**, 362-366.

35. J. de Melo, F. K. Hurtado, A. W. Prado, M. J. E. Souza and C. M. B. Rolim, *J. Liq. Chromatogr. Relat. Technol.*, 2008, **31**, 269-280.

36. J. A. Ardila, E. R. Sartori, R. C. Rocha-Filho and O. Fatibello-Filho, *Talanta*, 2013, **103**, 201-206.

37. E. P. Randviir, J. P. Metters, J. Stainton and C. E. Banks, *Analyst*, 2013, **138**, 2970-2981.

38. R. Pauliukaite, M. E. Ghica, O. Fatibello-Filho and C. M. A. Brett, *Electrochim. Acta*, 2010, **55**, 6239-6247.

39. D. K. Grosser, *Cyclic voltammetry simulation and analysis of raction mechanisms*, VCH Publisher, New York, 1994.

40. S. J. Konopka and B. McDuffie, *Anal. Chem.*, 1970, **42**, 1741-1746.

41. O. Ramdani, J. P. Metters, L. C. Figueiredo-Filho, O. Fatibello-Filho and C. E. Banks, *Analyst*, 2013, **138**, 1053-1059.

42. B. Razavi, W. H. Song, W. J. Cooper, J. Greaves and J. Jeong, *J. Phys. Chem. A*, 2009, **113**, 1287-1294.

43. E. Laviron, *J. Electroanal. Chem.*, 1979, **101**, 19-28.

44. J. C. Miller and J. N. Miller, *Statistics for analytical chemistry*, New York : Ellis Horwood PTR Prentice Hall, 1993.

Table 1.Comparison of the analytical parameters obtained using different methods for the determination of BZF in pharmaceutical formulations

Method	Concentration range (mol L^{-1})	LOD (mol L^{-1})	Reference
HPLC	$6.9 \times 10^{-7} - 1.4 \times 10^{-4}$	2.8×10^{-7}	32
HPLC	$2.8 \times 10^{-7} - 4.1 \times 10^{-5}$	–	33
HPLC	$5.5 \times 10^{-7} - 1.4 \times 10^{-4}$	2.8×10^{-8}	34
HPLC	$2.8 \times 10^{-6} - 1.4 \times 10^{-3}$	6.4×10^{-3}	35
Spectrophotometric	$6.9 \times 10^{-6} - 4.1 \times 10^{-5}$	1.2×10^{-6}	35
Voltammetric*	$1.0 \times 10^{-7} - 9.1 \times 10^{-6}$	9.8×10^{-8}	36
This work	$5.0 \times 10^{-8} - 9.1 \times 10^{-7}$	1.6×10^{-8}	This work

*Using Boron-doped diamond (BDD) electrode

Table 2. BZF content in pharmaceutical formulations (200 mg tablets) determined by the proposed SWAdSV method, using the MWCNT-DHP/GCE and a comparative spectrophotometric method

Sample	BZF (mg/tablet)		Average error[b] (%)
	Spectrophotometric	SWAdSV Method[a]	
A	212 ± 1	209 ± 2	–1.4
B	210 ± 2	204 ± 1	–2.9
C	209 ± 1	210 ± 2	0.5
D	211 ± 1	207 ± 1	–1.9

[a] Average of 3 measurements

[b] Average error = [100 × (SWAdSV Method – Spectrophotometric)] / Spectrophotometric

Figure captions

Figure 1. EIS diagrams for 1 mmol L^{-1} $K_4[Fe(CN)_6]$ in 0.1 mol L^{-1} KCl at the (a) GCE (b) MWCNT-DHP/GCE (c) DHP/GCE.

Figure 2. Cyclic adsorptive stripping voltammograms (v = 50 mV s^{-1}) for 30 μmol L^{-1} BZF in 0.1 mol L^{-1} phosphate buffer solution (pH 2.0) obtained using the bare GCE (solid line), DHP/GCE (short dotted line) and MWCNT-DHP/GCE (short dashed line). Adsorption time of 180 s.

Figure 3. Cyclic adsorptive stripping voltammograms (v = 50 mV s^{-1}) for 30 μmol L^{-1} BZF in 0.1 mol L^{-1} phosphate buffer solution at different pH values: (a) 5.0, (b) 4.0, (c) 3.0 and (d) 2.0. Adsorption time of 180 s. Insert: linear dependence of E_p with pH of the supporting electrolyte.

Figure 4. Proposed oxidation mechanism for BZF[36].

Figure 5. Linear sweep adsorptive stripping voltammograms for 30 μmol L^{-1} BZF in 0.1 mol L^{-1} phosphate buffer solution (pH 2.0) at different scan rates (ν): (a) 0.010, (b) 0.020, (c) 0.030, (d) 0.050, (e) 0.070, (f) 0.100, (g) 0.150, (h) 0.200 V s^{-1}. Adsorption time 180 s. Insert: linear dependence of E_p on ln ν.

Figure 6. Square-wave adsorptive stripping voltammograms in 0.1 mol L^{-1} phosphate buffer solution (pH 2.0) obtained using the MWCNT-DHP/GCE at different concentrations of BZF: (a) 0.0, (b) 50, (c) 70, (d) 100, (e) 190, (f) 290, (g) 380, (h) 470, (i) 560, (j) 650, (k) 740, (l) 820, (m) and 910 nmol L^{-1}. Adsorption time of 180 s. Insert: Corresponding analytical curve.

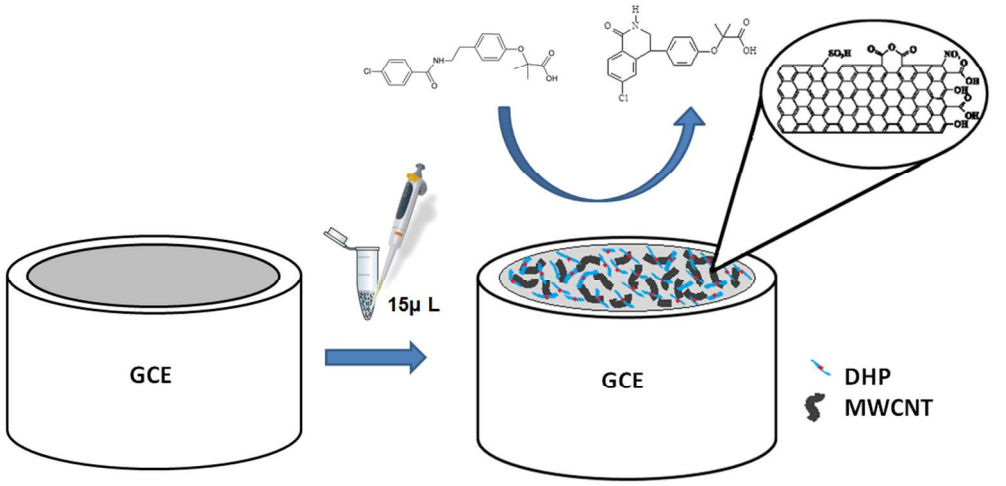

315x168mm (96 x 96 DPI)

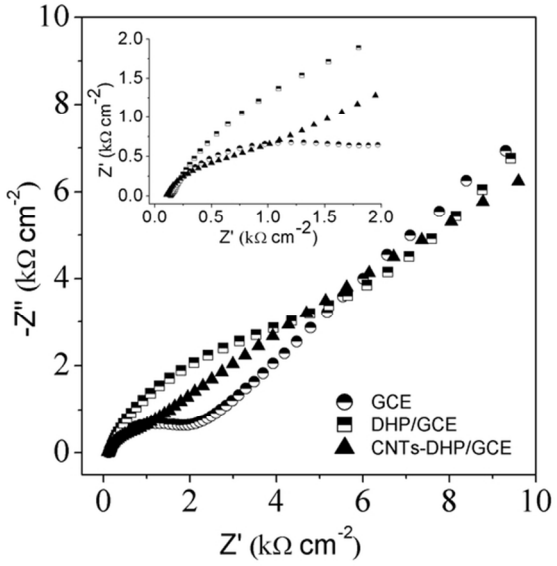

80x56mm (300 x 300 DPI)

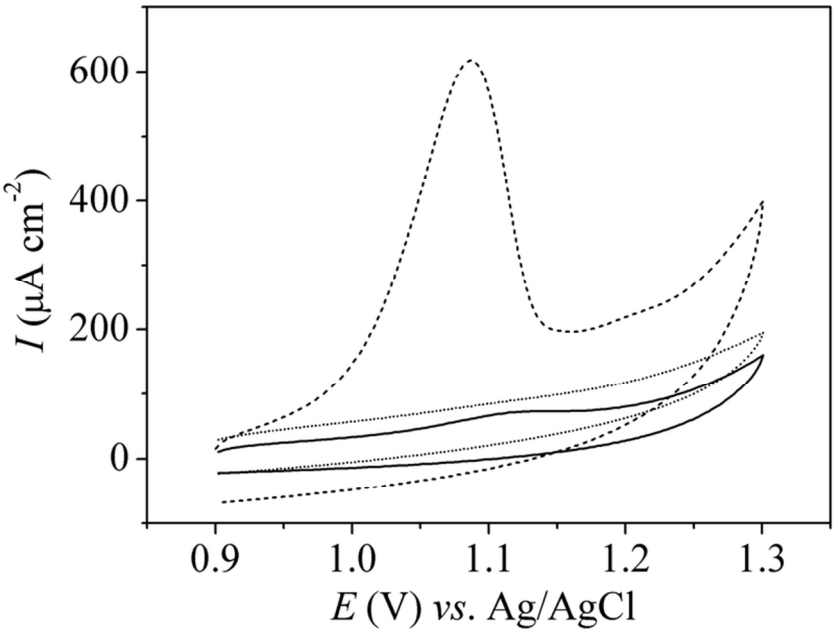

81x58mm (300 x 300 DPI)

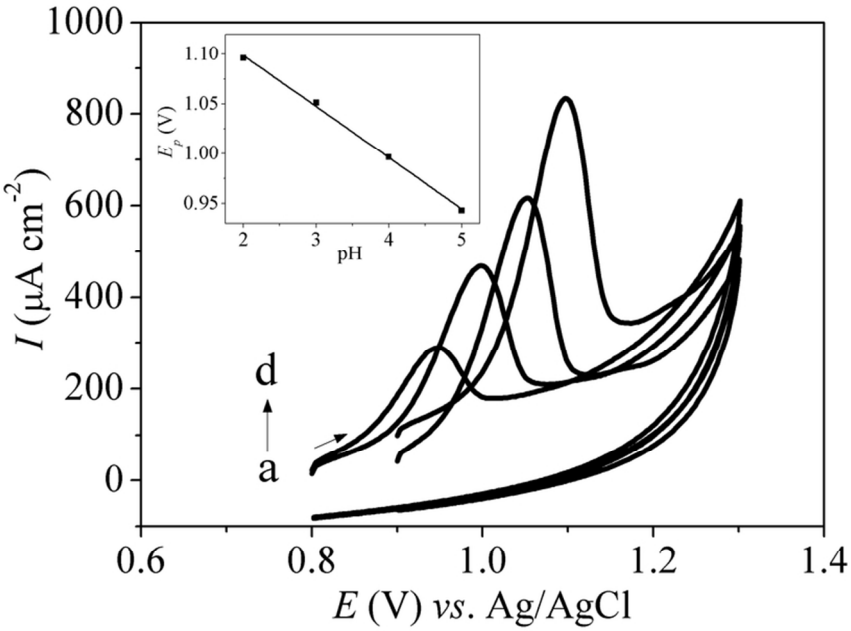

81x57mm (300 x 300 DPI)

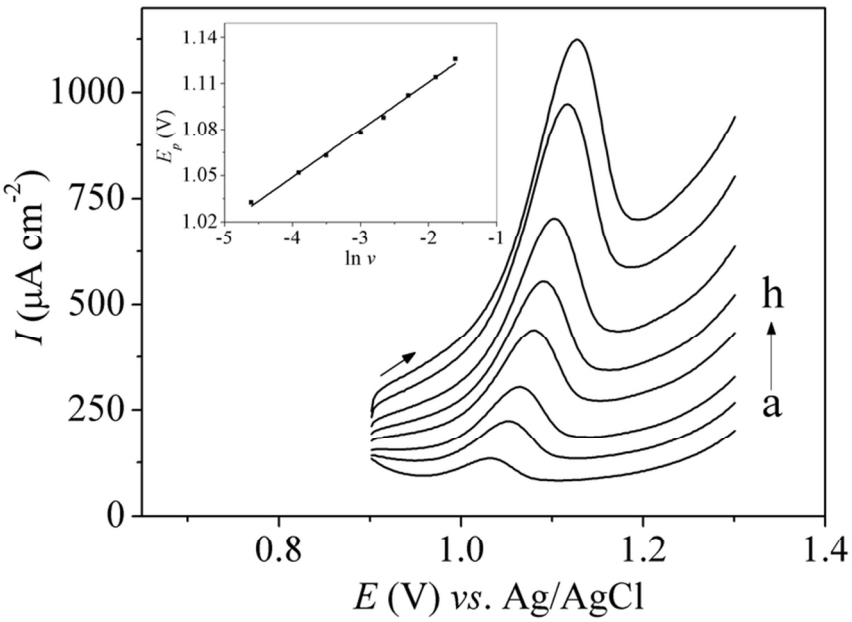

84x59mm (300 x 300 DPI)

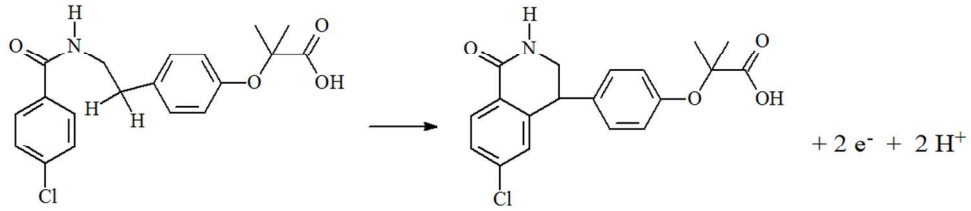

313x143mm (96 x 96 DPI)

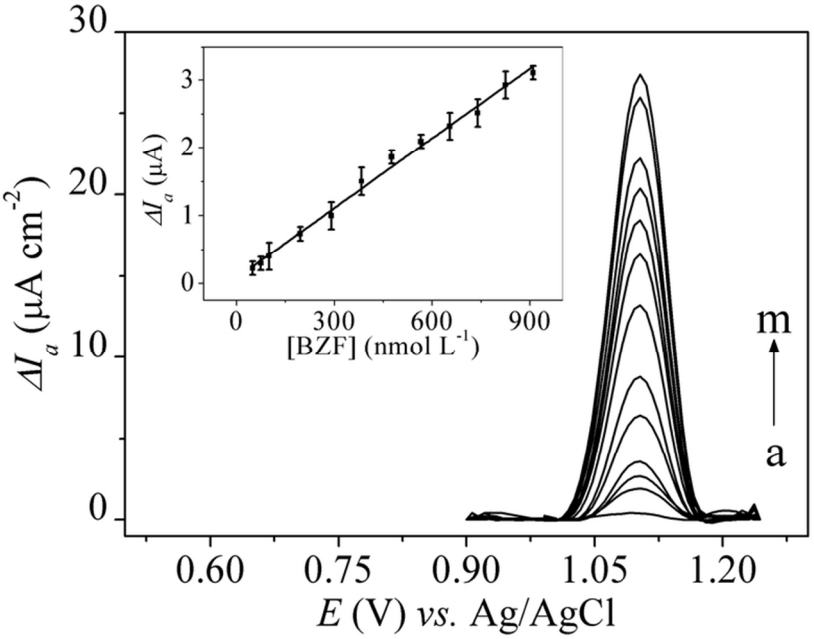

81x57mm (300 x 300 DPI)